AJNR

High Intravascular Signal Arterial Transit Time Artifacts Have Negligible Effects on Cerebral Blood Flow and Cerebrovascular Reserve Capacity Measurement Using Single Postlabel Delay Arterial Spin-Labeling in Patients with Moyamoya Disease

M. Fahlström, A. Lewén, P. Enblad, E.-M. Larsson and J. Wikström

AJNR Am J Neuroradiol 2020, 41 (3) 430-436
doi: https://doi.org/10.3174/ajnr.A6411
http://www.ajnr.org/content/41/3/430

High Intravascular Signal Arterial Transit Time Artifacts Have Negligible Effects on Cerebral Blood Flow and Cerebrovascular Reserve Capacity Measurement Using Single Postlabel Delay Arterial Spin-Labeling in Patients with Moyamoya Disease

M. Fahlström, A. Lewén, P. Enblad, E.-M. Larsson, and J. Wikström

ABSTRACT

BACKGROUND AND PURPOSE: Arterial spin-labeling-derived CBF values may be affected by arterial transit time artefacts. Thus, our aim was to assess to what extent arterial spin-labeling–derived CBF and cerebrovascular reserve capacity values in major vascular regions are overestimated due to the arterial transit time artifacts in patients with Moyamoya disease.

MATERIALS AND METHODS: Eight patients with Moyamoya disease were included before or after revascularization surgery. CBF maps were acquired using a 3D pseudocontinuous arterial spin-labeling sequence, before and 5, 15, and 25 minutes after an IV acetazolamide injection and were registered to each patient's 3D-T1-weighted images. Vascular regions were defined by spatial normalization to a Montreal Neurological Institute–based vascular regional template. The arterial transit time artifacts were defined as voxels with high signal intensity corresponding to the right tail of the histogram for a given vascular region, with the cutoff selected by visual inspection. Arterial transit time artifact maps were created and applied as masks to exclude arterial transit time artifacts on CBF maps, to create corrected CBF maps. The cerebrovascular reserve capacity was calculated as CBF after acetazolamide injection relative to CBF at baseline for corrected and uncorrected CBF values, respectively.

RESULTS: A total of 16 examinations were analyzed. Arterial transit time artifacts were present mostly in the MCA, whereas the posterior cerebral artery was generally unaffected. The largest differences between corrected and uncorrected CBF and cerebrovascular reserve capacity values, reported as patient group average ratio and percentage point difference, respectively, were 0.978 (95% CI, 0.968–0.988) and 1.8 percentage points (95% CI, 0.3–3.2 percentage points). Both were found in the left MCA, 15 and 5 minutes post-acetazolamide injection, respectively.

CONCLUSIONS: Arterial transit time artifacts have negligible overestimation effects on calculated vascular region-based CBF and cerebrovascular reserve capacity values derived from single-delay 3D pseudocontinuous arterial spin-labeling.

ABBREVIATIONS: ACA = anterior cerebral artery; ACZ = acetazolamide; ASL = arterial spin-labeling; ATT = arterial transit time; ATT_{over} = long arterial transit time where CBF is overestimated; ATT_{under} = very long arterial transit time where CBF is underestimated; CVRC = cerebrovascular reserve capacity; Diff = absolute difference; MMD = Moyamoya disease; PCA = posterior cerebral artery; pCASL = pseudocontinuous arterial spin-labeling; PLD = postlabeling delay; pp = percentage points

Moyamoya disease (MMD) is characterized by stenosis or occlusion at the terminal portions of the ICA, the proximal anterior cerebral arteries (ACAs), or the MCA. Common for patients with MMD is the presence of abnormal vascular networks in the arterial territories close to the stenotic or occlusive lesion.[1-3] Most patients can maintain adequate CBF through compensatory collateral flow, while others experience cerebral ischemia and hemorrhage.[1,4] The capability of the brain to increase CBF in response to a vasodilatory challenge can be assessed using cerebrovascular reserve capacity (CVRC) estimates, calculated as the maximal percentage increase in CBF after vasodilatory stimulus (commonly IV acetazolamide [ACZ], referred to as the ACZ challenge) relative to baseline.[4] CVRC can predict the risk of ischemic events in patients with MMD; moreover, CVRC can also provide information on indications for or assessment after cerebral revascularization surgery.[4,5]

Received September 29, 2019; accepted after revision December 24.

From the Departments of Surgical Sciences (M.F., E.-M.L., J.W.) and Neuroscience (A.L., P.E.), Uppsala University, Uppsala, Sweden.

Please address correspondence to Markus Fahlström, MSc, Department of Surgical Sciences, Uppsala University, Akademiska Sjukhuset, SE 751 85 Uppsala, Sweden; e-mail: Markus.Fahlstrom@radiol.uu.se

Indicates article with supplemental on-line tables.

Indicates article with supplemental on-line photos.

http://dx.doi.org/10.3174/ajnr.A6411

Arterial spin-labeling (ASL) is a completely noninvasive and highly repeatable perfusion imaging technique that has demonstrated potential in numerous cerebral disorders.[3,6,7] With ASL, quantification of CBF is possible using the patient's own blood as a freely diffusible tracer. One inherent limitation with single-delay pseudocontinuous ASL (pCASL) is the dependency on an arterial transit time (ATT; ie, the time for labeled blood to flow from the labeling plane to the tissue of interest), in which arterial transit time should not exceed the user-defined parameter, postlabeling delay (PLD). This limitation is known as the ATT artifact and have 2 different effects on the derived CBF maps, depending on to what extent the blood flow is delayed (ie, the length of the ATT). First, at a very long ATT, in which no blood has reached the imaging volume in time for the readout, derived CBF will be inherently low and underestimated (denoted "ATT_{under}"). Second, the ATT artifacts will appear as bright intravascular signal when the blood has reached the imaging volume but not the capillary bed—that is, it is found in precapillary arterioles, presenting as hyperintense areas in the derived CBF maps, thus overestimating CBF (denoted "ATT_{over}").[2,7-11] However, the ATT_{over} artifacts have been shown to provide important information about the presence and extent of collateral flow by visual grading in patients with MMD when long ATTs are present through collateral pathways.[2,3,9] No effort has been made to quantitatively define ATT_{over} artifacts, and their impact on CBF and CVRC calculations in major vascular regions, thus, testing the hypothesis that ATT_{over} has negligible effects on large ROIs.[8]

The aim of this study was to assess to what extent vascular region–based CBF and CVRC are affected by the ATT_{over} artifacts defined by means of histogram analysis.

MATERIALS AND METHODS

Patients

Eight patients with confirmed MMD were included before or after revascularization surgery. This study was performed in accordance with the Declaration of Helsinki and was approved by the local ethics committee. Patients were examined by MR imaging for pre- or postoperative assessment: monitoring the progression of the disease as a decision basis for an operation or postoperative follow-up assessing the surgical outcome, compared with preoperative assessment if available, both performed on a yearly basis or close to the scheduled operation. All patients received an intravenous injection with 1 g or 10 mg/kg of ACZ for adults and children, respectively.

MR Imaging Acquisition

All examinations were performed on an Achieva 3T scanner (Philips Healthcare, Best, the Netherlands) using a 32-channel head coil. High-resolution 3D T1-weighted and 3D T2-weighted FLAIR images were acquired as structural images. A commercially available 3D-pCASL sequence with a gradient and spin-echo readout module was used for acquiring CBF maps with a PLD of 2500 ms. The full set of acquisition parameters for all MR imaging sequences is presented in On-line Table 1. ASL-derived CBF maps were automatically calculated by the scanner according to the model defined by Buxton et al[12] and recommended by Alsop et al.[8] The standard ACZ challenge protocol included a total of 4 3D-pCASL acquisitions, performed before and 5, 15, and 25 minutes after the ACZ injection. Two examinations deviated from the above-described study protocol. For the first examination (the pilot), a work-in-progress 3D-pCASL sequence with a PLD of 2000 ms was performed before and 5, 10, and 15 minutes after ACZ injection. For the other examination, a work-in-progress 3D-pCASL sequence with a PLD of 2500 ms was performed with the standard ACZ challenge protocol described above. Because only 2 examinations at 10 minutes post-ACZ injections were performed, they were excluded from the statistical analysis.

Vascular Regions and Image Postprocessing

T2-weighted FLAIR images and CBF maps were coregistered to each subject's corresponding T1-weighted images. Gray matter probability maps were segmented from T1-weighted images and coregistered T2-weighted FLAIR images.[13] Gray matter maps were defined with a partial volume fraction above 75%. A deformation field, defining the transformation from Montreal Neurological Institute template space to subject-specific space for each subject, was derived on the basis of the subject's T1-weighted image and was applied to a standard vascular territory template,[14,15] including the bilateral ACA, MCA, and posterior cerebral artery (PCA). Each subject-specific vascular territory was masked with the corresponding gray matter map to correct for partial volume effects.[16-18] All processing steps, as described above, were performed using the SPM12 toolbox (http://www.fil.ion.ucl.ac.uk/spm/software/spm12).

Arterial Transit Time Artifact Correction

Arterial transit time artifacts (ATT_{over} artifacts) were defined as hyperintense spots and serpiginous regions in the right tail of the corresponding histogram of all vascular territory regions and for all CBF maps, respectively (Figs 1 and 2). The right tail segment corresponding to the ATT_{over} artifacts was selected, including histogram bins from right to left, thus always including the highest CBF values. The cutoff value was selected by visual inspection so that only voxels within the hyperintense spots were included, thus creating binary ATT_{over} maps. Furthermore, for each vascular region, ATT_{over} artifact volume and ATT_{over} artifact ratio (defined as ATT_{over} volume divided by total vascular region volume) were calculated.

CBF and CVRC Calculation

All uncorrected CBF maps were smoothed using a 5-mm Gaussian filter. Corrected CBF maps were created by masking uncorrected, smoothed CBF maps with corresponding ATT_{over} maps, thus excluding voxels defined as ATT_{over} artifacts from the statistical analysis. Corrected and uncorrected CBF values were extracted using previously defined vascular regions, respectively. CVRC values were calculated on the basis of regional CBF, using equation 1 for all post-ACZ-acquired corrected and uncorrected CBF maps, respectively, with corresponding $CBF^{0\ minute}$ defining baseline. Furthermore, the absolute difference (Diff) in percentage points between the corrected and uncorrected CVRC was calculated. Super- and subscript will be used to clarify ratios and to distinguish between baseline (0 min) and post-ACZ injection (5 min and so forth), eg, $CBF^{5\ min}_{Ratio}$ or $CVRC^{5\ min}_{Diff}$ when applicable.

1) $$CVRC = (CBF^{post-ACZ} - CBF^{0\ minute})/(CBF^{0\ minute})$$

Statistical Analysis

For descriptive analysis of ATT_{over} volume and ATT_{over} ratio, mean, maximum value, and 95% CI were calculated. Furthermore, CBF and CVRC comparisons were performed by descriptive analysis of the corrected-to-uncorrected ratio (CBF) or the absolute difference in percentage points (CVRC); thus, the average ratio/difference with 95% CI and maximum/minimum were calculated and analyzed. Descriptive analysis was performed for all vascular regions and baseline and 5 , 15, and 25 minutes post-ACZ injection, respectively. A correlation analysis was peformed comparing the CBF_{Ratio} with ATT volume using the Pearson correlation coefficient. This was performed using all time point values as 1 large dataset. Derived *P* values are presented as exact values and are 2-sided, and $P < .05$ is considered significant. GraphPad Prism 8 for Mac (GraphPad Software, San Diego, California) was used for statistical analysis and graph design.

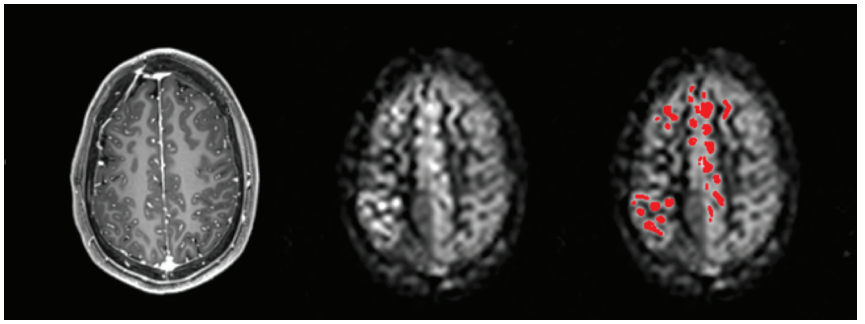

FIG 1. A 3D TI-weighted image with derived CBF maps with and without binary ATT_{over} voxels (red).

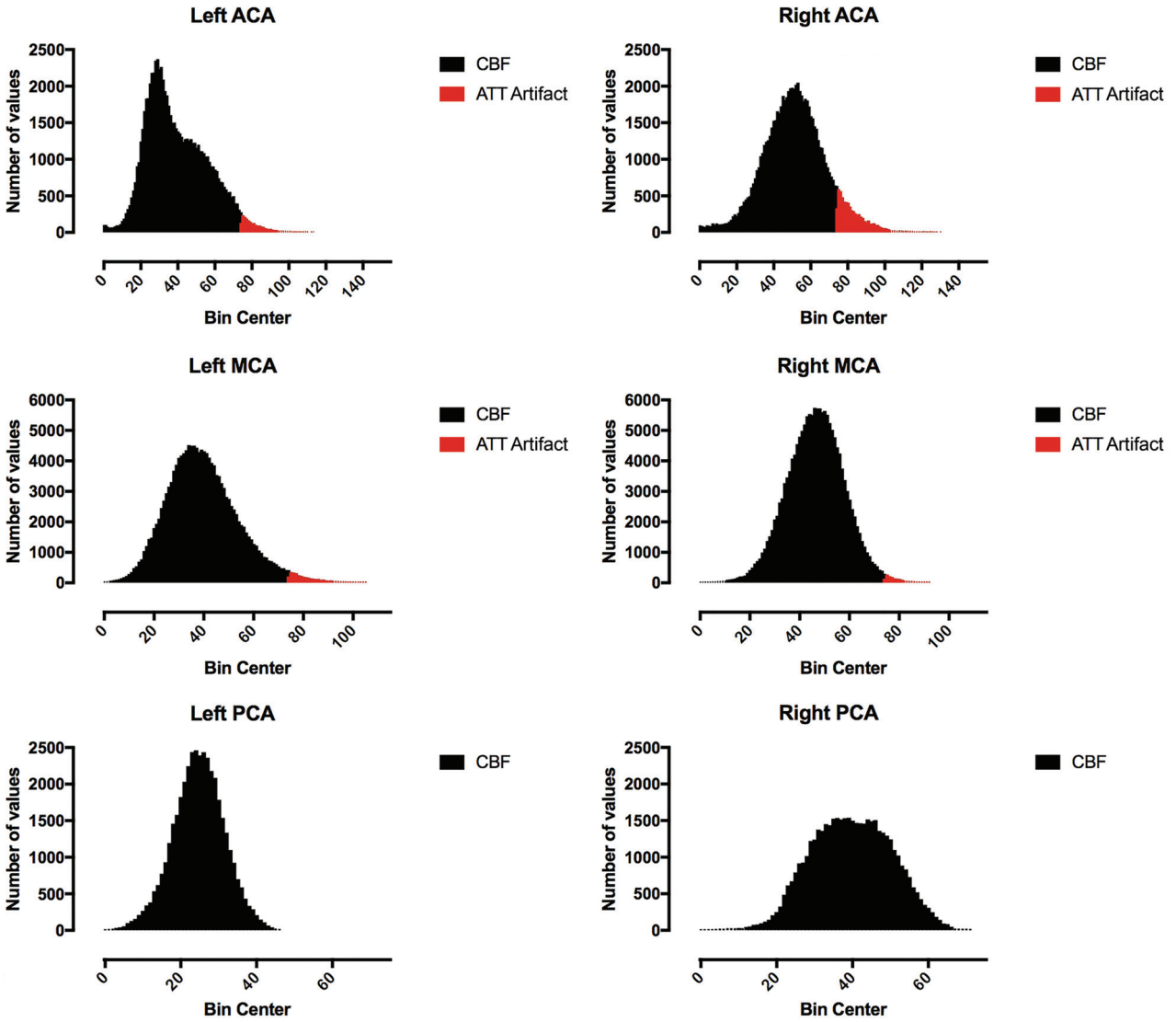

FIG 2. Derived histograms and defined ATT_{over} voxels from the CBF maps presented in Fig 1.

Table 1: Average of derived ratios, minimum/maximum, and 95% CI for CBF_{Ratio}

CBF_{Ratio}	ACA		MCA		PCA	
	Left	Right	Left	Right	Left	Right
Baseline						
Mean	0.989	0.986	0.979	0.980	0.995	0.996
95% CI	0.981–0.995	0.978–0.994	0.971–0.988	0.972–0.987	0.990–1.000	0.992–1.001
Min-max	0.949–1.000	0.942–1.000	0.954–1.000	0.958–0.999	0.961–1.000	0.970–1.000
5 minutes						
Mean	0.991	0.987	0.981	0.978	0.992	0.992
95% CI	0.986–0.991	0.980–0.995	0.975–0.988	0.970–0.986	0.985–0.999	0.985–0.999
Min-max	0.975–0.999	0.955–0.998	0.961–0.998	0.950–0.998	0.956–1.000	0.952–1.000
15 minutes						
Mean	0.990	0.987	0.981	0.979	0.995	0.996
95% CI	0.983–0.997	0.980–0.993	0.973–0.988	0.970–0.987	0.992–0.998	0.993–0.999
Min-max	0.948–0.999	0.957–0.999	0.937–0.998	0.942–0.997	0.980–1.000	0.982–1.000
25 minutes						
Mean	0.989	0.985	0.980	0.978	0.995	0.997
95% CI	0.981–0.998	0.977–0.993	0.970–0.990	0.968–0.988	0.991–0.999	0.994–1.000
Min-max	0.943–1.000	0.960–1.000	0.938–0.996	0.944–0.997	0.976–1.000	0.982–1.000

Note:—Min-max indicates minimum-maximum.

Table 2: Average of derived differences, maximum, and 95% CI for $CVRC_{Diff}$

$CVRC_{Diff}$ (pp)	ACA		MCA		PCA	
	Left	Right	Left	Right	Left	Right
5 minutes						
Mean	0.7	1.1	1.8	1.7	0.8	1.5
95% CI	0.3–1.0	0.4–1.7	0.3–3.2	0.9–2.6	0.1–1.6	−0.5–3.1
Maximum	2.2	4.2	11.3	5.9	5.2	7.8
15 minutes						
Mean	0.8	1.1	0.9	1.5	0.9	0.8
95% CI	0.3–1.2	0.4–1.7	0.4–1.5	0.6–2.3	−0.2–1.9	−0.2–1.9
Maximum	3.5	4.5	3.1	5.4	6.7	6.8
25 minutes						
Mean	1.0	1.3	1.7	1.5	0.3	0.4
95% CI	0.4–1.7	0.4–2.2	0.5–2.9	0.7–2.3	0.0–0.5	−0.2–1.1
Maximum	4.1	5.5	5.8	4	0.9	3.3

RESULTS

Patients

A total of 16 examinations were performed, which included 9 preoperative and 7 postoperative examinations. Two patients had both pre- and postoperative examinations.

ATT_{over} Volume

A representative example of ATT_{over} artifact definition can be seen in Figs 1 and 2. For all examinations, arranged by post-ACZ injection time points, descriptive statistics for bilateral ACA, MCA, and PCA are presented in On-line Table 2 and On-line Fig 1. The largest ATT_{over} artifact volume was 30.9 cm^3 (left MCA at 25 minutes post-ACZ injection). Generally, ATT_{over} artifacts were mostly present in the MCA, while the PCA was mostly unaffected; furthermore, the volumes typically increased from baseline compared with post-ACZ injection.

Comparison of CBF Values

The average CBF_{Ratio} was generally close to 1.0, with a narrow 95% CI, considering all major vascular regions including ACZ challenges, thus suggesting minor differences between corrected and uncorrected CBF. The smallest calculated CBF_{Ratio} was 0.937 (corrected CBF, 51.16 mL/100 g/min, and uncorrected, 54.61 mL/100 g/min in the left MCA at 15 minutes post-ACZ injection)—that is, the largest difference found between any corrected and uncorrected CBF values was 6.3% (Table 1 and On-line Fig 2). The correlation between the CBF_{Ratio} and ATT volume was negative and strong ($r = -0.85$, $P < .001$, On-line Fig 3).

Comparison of CVRC Values

For all major vascular regions, including ACZ challenges, the calculated average $CVRC_{Diff}$ was small, with a narrow 95% CI (highest $CVRC_{Diff}$ average, 1.8 percentage points [pp]; 95% CI, 0.3–3.2 pp; On-line Fig 4). The maximum $CVRC_{Diff}$ was 11.3 pp (the corrected CVRC was 46.2% and the uncorrected CVRC was 34.9% in the left MCA at 5 minutes post-ACZ injection, Table 2).

DISCUSSION

This study assessed the extent of the ATT_{over} artifacts, presenting as hyperintense spots on single-delay ASL acquisitions during ACZ challenges in patients with MMD, and the effect of the ATT_{over} artifacts on CBF and CVRC values in major vascular territories. Major findings included the following: In major vascular territories, the ATT_{over} artifacts have negligible effects on derived CBF and CVRC values.

The anterior circulation is predominantly affected in patients with MMD;[1,4,9] furthermore, no patient in our study had any occlusion affecting the PCA. This finding agrees with the derived distribution of average ATT_{over} volume in the bilateral major vascular territories used in this study.

Comparing corrected and uncorrected CBF values, we found small, negligible differences. Alsop et al[8] suggested that CBF measurements may still be valid in large ROIs in the presence of ATT_{over} if flow-crushing gradients are not used. The results of this study prove this hypothesis valid for major vascular regions in patients with MMD. Furthermore, because CVRC is an

imperative prognostic factor for assessing and evaluating patients with MMD pre- and postsurgery,[4,5] assessing how CVRC is affected by the ATT_{over} artifacts is of great importance. We found generally small, negligible percentage point differences between corrected and uncorrected CVRC. The maximum difference was 11.3 pp (corrected CVRC, 46.2%; and uncorrected CVRC, 34.9%). In this case, the difference was found at 5 minutes post-ACZ injection, a time point not commonly used during ACZ challenges and CVRC calculation.[4,19-24] We also assessed possible correlations between CBF_{Ratio} and ATT_{over} volume and found a strong, significant negative correlation ($r = -0.85$, $P < .001$). This is expected; as we exclude more pixel values with increasing ATT volume, the effect on average corrected mean CBF would inherently be larger. However, we do not consider this relationship to be a potential bias.

In a quantitative regional analysis comparing multidelay pulsed ASL with DSC MR imaging, Martin et al[25] found a moderate correlation for normalized CBF, which increased slightly after exclusion of ATT_{over} in the MCA region. It is inherently difficult to compare these results with ours because important inconsistencies between the studies exist. The study by Martin et al was primarily designed to compare a multidelay pulsed ASL with DSC MR imaging in patients with unilateral atherosclerotic stenoocclusive disease. CBF was normalized to contralateral vascular regions not affected by occlusion, and pulsed ASL has a lower achievable SNR compared with pCASL. Multidelay ASL has been proposed as an imaging technique for patients with MMD, due to mainly 1 advantage: less vulnerability to ATT artifacts. On the other hand, single-delay ASL has signal-to-noise and scan time advantages over multidelay ASL,[26] and the results presented here should be considered favorable for single-delay ASL.

We acquired CBF measurements 5, 15, and 25 minutes post-ACZ injection. While the ATT_{over} volume increased post-ACZ injection, there were no pronounced effects on either CBF or CVRC. The increase in ATT_{over} volume is expected, considering the reported increase in MTT derived from perfusion CT post-ACZ injection, especially in regions supplied by occluded vessels.[4,27] However, Federau et al[21] showed that ATT estimates based on multidelay ASL–acquired data decreased after injection of ACZ.

The current reference standard for CBF measurements (and thus CVRC) is ^{15}O-water PET.[9,24] ^{15}O-water PET requires, however, an on-site cyclotron, and the availability is limited.[9] SPECT is more readily available and is frequently used for MMD evaluation, but with limitations such as poor spatial resolution.[24,28] In addition, both PET and SPECT imaging are invasive and expose the patient to ionizing radiation.[2,5,9,23,29] Consequently, assessing the correlation between ASL-derived CBF and CBF derived from PET and SPECT is important, and this has been studied extensively. High correlations have been reported between SPECT (^{123}I-iodoamphetamine and ^{99m}Tc-hexamethylpropyleneamine oxime) and ASL (different sequences, PLDs, and field strengths).[5,23,24,30] The dependency of the PLD as a parameter affecting correlation with ^{15}O-water PET has been highlighted by others. Hara et al[29] concluded that ASL acquired with a short PLD (1525 ms) showed better correlation with ^{15}O-gas PET in normally perfused areas compared with a long PLD (2525 ms) in patients with MMD. However, in symptomatic areas, where arterial transit is delayed, correlation increased for a long PLD and was then higher than a short PLD. The importance of the PLD was furthermore highlighted in a study by Inoue et al,[6] presenting different CVRC values in healthy volunteers depending on the PLD. In a comparative study using simultaneously acquired ASL and ^{15}O-water PET, Fan et al[9] concluded that long PLDs (4000 ms, compared with our PLD of 2500 ms) are needed to achieve good correlations between relative CBF measurements in patients with MMD.

Another limitation addressed by the authors is the lack of acquired arterial blood samples to enable absolute CBF from kinetic modeling of the PET data. Arterial blood samples were not collected, as stated by the authors, to minimize patient discomfort. Goetti et al[31] also reported good correlations in children and young adults with MMD between ASL and ^{15}O-water PET; however, data were not acquired simultaneously, with a short PLD of 1500 ms and after normalization to cerebellar CBF-values. Again, no arterial blood samples were collected. This feature is an important limitation with ^{15}O-water PET; quantitative studies require an arterial input function most reliably acquired through continuous arterial sampling.[32,33] Arterial sampling may not be feasible in patients in poor condition and is not feasible in children with MMD.[33] However, several noninvasive methods can estimate relative CBF in the absence of existing arterial blood sampling.[33,34] ASL is, by definition, fully noninvasive, with no radiation exposure and greater availability than cyclotron-dependent ^{15}O-water PET. As concluded by other authors, ASL-derived CBF/CVRC has potential in pre-/postoperative assessment in patients with MMD.[3,5,6,9,24-26,29,31,35-37]

Limitations

In the histogram analysis, the right tail cutoff value defining the ATT_{over} artifacts was selected by visual inspection. A manual approach with only 1 reader is generally considered a limitation due to the dependency on the reader's ability to achieve high specificity. However, the histogram analysis method appeared robust, and the highest CBF values were always included because the selection of the ATT_{over} segment of the histogram was performed from right to left; thus, we do not consider this to confound our results.

Another drawback of our study was that we did not have a sufficient imaging slab to cover the whole brain, including the cerebellum, which has been used for normalization in several publications.[2,24,29,31] However, cerebellar normalization is not commonly performed, and CVRC is, by definition, a ratio; thus, we do not expect this to affect our results.

Two ACZ challenges were performed with a work-in-progress 3D-pCASL sequence with PLDs of 2000 and 2500 ms, respectively. These examinations were not excluded from this study and were not different from the others in regard to the derived CBF_{Ratio} and $CVRC_{Diff}$.

In the present study, no effort was made to assess whether the presence of ATT_{under} artifacts would affect our results. Given the theory of ATT artifacts as outlined in the introduction, the presence of ATT_{over} artifacts could indicate that possible surrounding regional hypoperfusion can be a consequence of ATT_{under} artifacts. Still, we are analyzing ratio-based data, and given that both corrected and uncorrected CBF maps would have the same extent

for the ATT_{under} artifacts, we consider this to have a minor impact on our results and conclusions. Moreover, the use of a long PLD in this study will reduce the ATT_{under} artifacts as reported by Hara et al.[29]

Partial volume effects are caused by the limited spatial resolution in ASL and tend to result in under- and overestimation of CBF in the GM and WM, respectively.[17,38] We used a simple partial volume correction method, masking all vascular regions with a GM mask. Furthermore, to reduce any registration errors between pre- and post-ACZ ASL acquisitions, we applied a Gaussian filter of 5 mm before ATT_{over} correction.[5,20,31,35]

We argue that single-delay ASL still has potential for this patient population. We also argue that ASL, in general, should be considered an excellent method for clinical assessment in patients with MMD. ASL allows us to capture the dynamic response[6] and further explore the clinical implications of the ACZ challenge in patients with MMD. Still, further studies are needed to evaluate single-delay and as well as multidelay ASL as a complete substitute for other, invasive, not readily available, ionizing radiation–based methods.

CONCLUSIONS

ATT_{over} artifacts, defined by means of histogram analysis, have negligible effects on calculated CBF and CVRC derived from single-delay 3D-pCASL while suppressing ATT_{under} using a long PLD. Major vascular regions are large enough for CBF and CVRC to be valid, thus making single-delay 3D-pCASL a valuable tool in pre- and postoperative assessment of patients with MMD.

REFERENCES

1. Kuroda S, Houkin K. **Moyamoya disease: current concepts and future perspectives.** *Lancet Neurol* 2008;7:1056–66 CrossRef Medline
2. Lee S, Yun TJ, Yoo RE, et al. **Monitoring cerebral perfusion changes after revascularization in patients with Moyamoya disease by using arterial spin-labeling MR imaging.** *Radiology* 2018;288:565–72 CrossRef Medline
3. Zaharchuk G, Do HM, Marks MP, et al. **Arterial spin-labeling MRI can identify the presence and intensity of collateral perfusion in patients with Moyamoya disease.** *Stroke* 2011;42:2485–91 CrossRef Medline
4. Vagal AS, Leach JL, Fernandez-Ulloa M, et al. **The acetazolamide challenge: techniques and applications in the evaluation of chronic cerebral ischemia.** *AJNR Am J Neuroradiol* 2009;30:876–84 CrossRef Medline
5. Noguchi T, Kawashima M, Nishihara M, et al. **Noninvasive method for mapping CVR in Moyamoya disease using ASL-MRI.** *Eur J Radiol* 2015;84:1137–43 CrossRef Medline
6. Inoue Y, Tanaka Y, Hata H, et al. **Arterial spin-labeling evaluation of cerebrovascular reactivity to acetazolamide in healthy subjects.** *AJNR Am J Neuroradiol* 2014;35:1111–16 CrossRef Medline
7. Zaharchuk G. **Arterial spin-labeling for acute stroke: practical considerations.** *Transl Stroke Res* 2012;3:228–35 CrossRef Medline
8. Alsop DC, Detre JA, Golay X, et al. **Recommended implementation of arterial spin-labeled perfusion MRI for clinical applications: a consensus of the ISMRM Perfusion Study Group and the European Consortium for ASL in Dementia.** *Magn Reson Med* 2015;73:102–16 CrossRef Medline
9. Fan AP, Guo J, Khalighi MM, et al. **Long-delay arterial spin labeling provides more accurate cerebral blood flow measurements in Moyamoya patients: a simultaneous positron emission tomography/MRI study.** *Stroke* 2017;48:2441–49 CrossRef Medline
10. Mutke MA, Madai VI, von Samson-Himmelstjerna FC, et al. **Clinical evaluation of an arterial-spin-labeling product sequence in steno-occlusive disease of the brain.** *PLoS One* 2014;9:e87143 CrossRef Medline
11. Chng SM, Petersen ET, Zimine I, et al. **Territorial arterial spin labeling in the assessment of collateral circulation: comparison with digital subtraction angiography.** *Stroke* 2008;39:3248–54 CrossRef Medline
12. Buxton RB, Frank LR, Wong EC, et al. **A general kinetic model for quantitative perfusion imaging with arterial spin-labeling.** *Magn Reson Med* 1998;40:383–96 CrossRef Medline
13. Lindig T, Kotikalapudi R, Schweikardt D, et al. **Evaluation of multimodal segmentation based on 3D T1-, T2- and FLAIR-weighted images: the difficulty of choosing.** *Neuroimage* 2018;170:210–21 CrossRef Medline
14. Mutsaerts HJ, van Dalen JW, Heijtel DF, et al. **Cerebral perfusion measurements in elderly with hypertension using arterial-spin labeling.** *PLoS One* 2015;10:e0133717 CrossRef Medline
15. Tatu L, Moulin T, Bogousslavsky J, et al. **Arterial territories of the human brain: cerebral hemispheres.** *Neurology* 1998;50:1699–1708 CrossRef Medline
16. Chen Y, Wang DJ, Detre JA. **Test-retest reliability of arterial spin-labeling with common labeling strategies.** *J Magn Reson Imaging* 2011;33:940–49 CrossRef Medline
17. Petr J, Schramm G, Hofheinz F, et al. **Partial volume correction in arterial spin-labeling using a Look-Locker sequence.** *Magn Reson Med* 2013;70:1535–43 CrossRef Medline
18. Wu WC, Jiang SF, Yang SC, et al. **Pseudocontinuous arterial spin labeling perfusion magnetic resonance imaging: a normative study of reproducibility in the human brain.** *Neuroimage* 2011;56:1244–50 CrossRef Medline
19. Andaluz N, Choutka O, Vagal A, et al. **Patient selection for revascularization procedures in adult Moyamoya disease based on dynamic perfusion computerized tomography with acetazolamide challenge (PCTA).** *Neurosurg Rev* 2010;33:225–32; discussion 232–33 CrossRef Medline
20. Detre JA, Samuels OB, Alsop DC, et al. **Noninvasive magnetic resonance imaging evaluation of cerebral blood flow with acetazolamide challenge in patients with cerebrovascular stenosis.** *J Magn Reson Imaging* 1999;10:870–75 CrossRef Medline
21. Federau C, Christensen S, Zun Z, et al. **Cerebral blood flow, transit time, and apparent diffusion coefficient in Moyamoya disease before and after acetazolamide.** *Neuroradiology* 2017;59:5–12 CrossRef Medline
22. Ni WW, Christen T, Rosenberg J, et al. **Imaging of cerebrovascular reserve and oxygenation in Moyamoya disease.** *J Cereb Blood Flow Metab* 2017;37:1213–22 CrossRef Medline
23. Noguchi T, Kawashima M, Irie H, et al. **Arterial spin-labeling MR imaging in moyamoya disease compared with SPECT imaging.** *Eur J Radiol* 2011;80:e557–62 CrossRef Medline
24. Yun TJ, Paeng JC, Sohn CH, et al. **Monitoring cerebrovascular reactivity through the use of arterial spin labeling in patients with Moyamoya disease.** *Radiology* 2016;278:205–13 CrossRef Medline
25. Martin SZ, Madai VI, von Samson-Himmelstjerna FC, et al. **3D GRASE pulsed arterial spin labeling at multiple inflow times in patients with long arterial transit times: comparison with dynamic susceptibility-weighted contrast-enhanced MRI at 3 Tesla.** *J Cereb Blood Flow Metab* 2015;35:392–401 CrossRef Medline
26. Donahue MJ, Achten E, Cogswell PM, et al. **Consensus statement on current and emerging methods for the diagnosis and evaluation of cerebrovascular disease.** *J Cereb Blood Flow Metab* 2018;38:1391–1417 CrossRef Medline
27. Eskey CJ, Sanelli PC. **Perfusion imaging of cerebrovascular reserve.** *Neuroimaging Clin N Am* 2005;15:367–81, xi CrossRef Medline

28. Lee M, Zaharchuk G, Guzman R, et al. **Quantitative hemodynamic studies in Moyamoya disease: a review.** *Neurosurg Focus* 2009;26:E5 CrossRef Medline
29. Hara S, Tanaka Y, Ueda Y, et al. **Noninvasive evaluation of CBF and perfusion delay of Moyamoya disease using arterial spin-labeling MRI with multiple postlabeling delays: comparison with (15)O-Gas PET and DSC-MRI.** *AJNR Am J Neuroradiol* 2017;38:696–702 CrossRef Medline
30. Sugino T, Mikami T, Miyata K, et al. **Arterial spin-labeling magnetic resonance imaging after revascularization of Moyamoya disease.** *J Stroke Cerebrovasc Dis* 2013;22:811–16 CrossRef Medline
31. Goetti R, Warnock G, Kuhn FP, et al. **Quantitative cerebral perfusion imaging in children and young adults with Moyamoya disease: comparison of arterial spin-labeling-MRI and H(2)[(15)O]-PET.** *AJNR Am J Neuroradiol* 2014;35:1022–28 CrossRef Medline
32. Boellaard R, van Lingen A, van Balen SC, et al. **Characteristics of a new fully programmable blood sampling device for monitoring blood radioactivity during PET.** *Eur J Nucl Med* 2001;28:81–89 CrossRef Medline
33. Koopman T, Yaqub M, Heijtel DF, et al. **Semi-quantitative cerebral blood flow parameters derived from non-invasive [(15)O]H2O PET studies.** *J Cereb Blood Flow Metab* 2019;39:163–72 CrossRef Medline
34. Khalighi MM, Deller TW, Fan AP, et al. **Image-derived input function estimation on a TOF-enabled PET/MR for cerebral blood flow mapping.** *J Cereb Blood Flow Metab* 2018;38:126–35 CrossRef Medline
35. Blauwblomme T, Lemaitre H, Naggara O, et al. **Cerebral blood flow improvement after indirect revascularization for pediatric Moyamoya disease: a statistical analysis of arterial spin-labeling MRI.** *AJNR Am J Neuroradiol* 2016;37:706–12 CrossRef Medline
36. Wang R, Yu S, Alger JR, et al. **Multi-delay arterial spin labeling perfusion MRI in Moyamoya disease–comparison with CT perfusion imaging.** *Eur Radiol* 2014;24:1135–44 CrossRef Medline
37. Choi HJ, Sohn CH, You SH, et al. **Can arterial spin-labeling with multiple postlabeling delays predict cerebrovascular reserve?** *AJNR Am J Neuroradiol* 2018;39:84–90 CrossRef Medline
38. Ahlgren A, Wirestam R, Lind E, et al. **A linear mixed perfusion model for tissue partial volume correction of perfusion estimates in dynamic susceptibility contrast MRI: impact on absolute quantification, repeatability, and agreement with pseudo-continuous arterial spin labeling.** *Magn Reson Med* 2017;77:2203–14 CrossRef Medline